ELSEVIER

Journal of Power Sources 113 (2003) 329–334

JOURNAL OF POWER SOURCES

www.elsevier.com/locate/jpowsour

# In situ EC-AFM observation with atomic resolution of Pb(1 0 0) and Pb(1 1 1) single crystals in sulfuric acid solution

Nobumitsu Hirai[a,*], Kimiyoshi Takeda[a], Shigeta Hara[a], Masashi Shiota[a,b], Yoshiaki Yamaguchi[b], Yasuhide Nakayama[b]

[a]*Department of Material Science and Processing, Faculty of Engineering, Graduate School of Engineering, Osaka University, Yamadaoka 2-1, Suita, Osaka 565-0871, Japan*

[b]*Yuasa Corporation, 2-3-21 Kosobe-cho, Takatsuki, Osaka 569-1115, Japan*

**Abstract**

Pb(1 0 0) and Pb(1 1 1) single crystals in 50 mM $H_2SO_4$ aqueous solution have been investigated by in situ electrochemical atomic force microscopy (EC-AFM) under potential control. We have succeeded in observating high resolution images of Pb(1 0 0) and Pb(1 1 1) single crystals, as well as high resolution and morphological images of $PbSO_4$ crystals formed on the Pb single crystals. We found that the top face of $PbSO_4$ crystals formed on Pb(1 0 0) is $PbSO_4$(0 0 1), while that on Pb(1 1 1) is $PbSO_4$(1 0 0). We also found that the atomic rows along the [1 0 0] and [0 1 0] direction of $PbSO_4$(0 0 1) surface were parallel with those along the [0 1 1] and [0 1 $\bar{1}$] direction of the Pb(1 0 0) substrate, while those along the [0 1 0] and [0 0 1] direction of the $PbSO_4$ (1 0 0) surface were parallel with those along the [0 1 $\bar{1}$] and [$\bar{1}$ 1 1] direction of the Pb(1 1 1) substrate.



*Keywords:* Atomic force microscopy; Lead–acid batteries; Negative electrodes; Surface structure; Morphology; Roughness; Topography; Lead; Metal–electrolyte interface

## 1. Introduction

The behavior of Pb electrodes in sulfuric acid solution is very important from both scientific and practical viewpoints because it closely relates to the electrochemical reaction on the negative electrode of lead–acid batteries. Electrochemical atomic force microscopy (EC-AFM), as well as electrochemical scanning tunneling microscopy (EC-STM), is one of the powerful tools, which can observe the morphology of the electrode surfaces in electrolyte. Remarkable knowledge about the electrochemical reactions on the negative and positive electrodes of lead–acid batteries has been obtained through our EC-AFM observation of the morphological changes on Pb and $PbO_2$ electrodes in sulfuric acid solution during oxidation and reduction [1–5].

On the other hand, EC-AFM and EC-STM can also observe atomic or molecular arrangements on single crystals of noble metals in electrolyte [6,7]. However, there are few atomic resolution EC-AFM or EC-STM observations of the electrodes of base metals, such as nickel [8,9], cobalt [10], iron [11], lead [12], and so on, because it is generally difficult to remove the surface oxide layer formed in air. In this paper, we have investigated the in situ EC-AFM observations of Pb(1 0 0) and Pb(1 1 1) single crystals in sulfuric acid solution under potential control.

## 2. Experimental

The samples used are Pb(1 0 0) and Pb(1 1 1) single crystals (MaTecK Co.). Immediately before the EC-AFM observation, the samples were polished chemically with a mixed solution of acetic acid and hydrogen peroxide and were washed finally with ethanol. The EC-AFM used is a Nanoscope IIIa (Digital Instruments). Fig. 1 shows the cross-section of EC-AFM cell. The potential of working electrode was controlled by a potentiostat and was referred to the reference electrode. The reference electrode used here was the $Hg/Hg_2SO_4$ electrode (0.65 V versus normal hydrogen electrode; NHE), to which all potential was referred in this paper. The space surrounded by the working electrode, the cantilever mount and the O-ring was filled with the electrolytes. The electrolytes used here were 50 mM $H_2SO_4$ aqueous solution, which were prepared from $H_2SO_4$ (Wako,

* Corresponding author. Tel.: +81-6-879-7467; fax: +81-6-879-7467.
*E-mail address:* nhirai@mat.eng.osaka-u.ac.jp (N. Hirai).

0378-7753/02/$ – see front matter 
PII: S0378-7753(02)00545-1

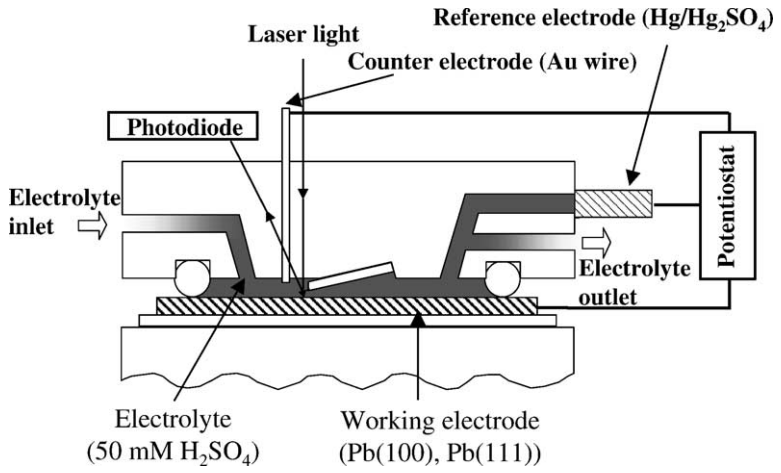


Fig. 1. Schematic illustration of cross-section of EC-AFM electrochemical cell.

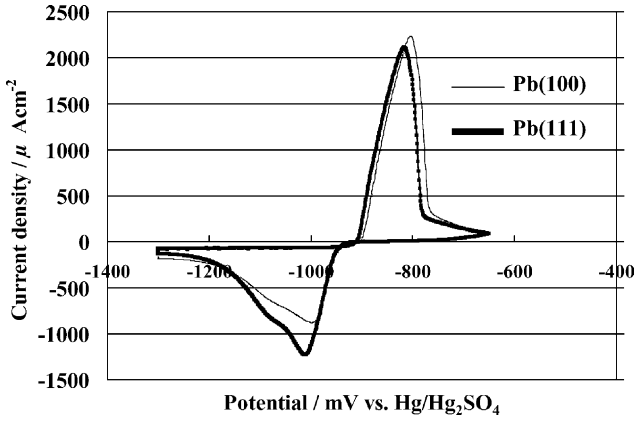


Fig. 2. Cyclic voltammogram for Pb(1 0 0) and Pb(1 1 1) in 50 mM $H_2SO_4$ solution with sweep rate of 1 mV $s^{-1}$.

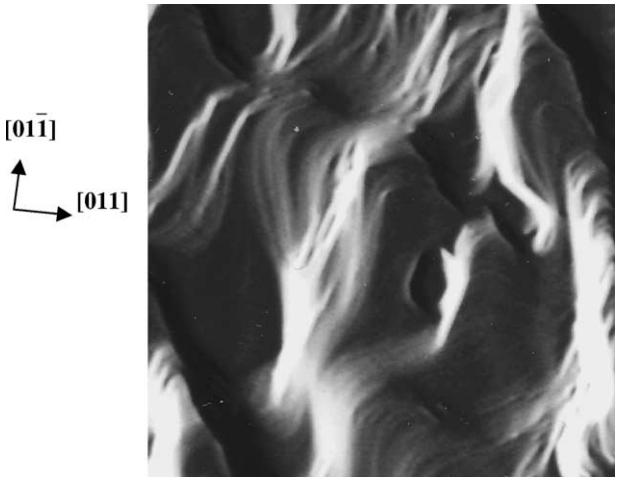


Fig. 3. EC-AFM morphological image (5 μm × 5 μm) on Pb(1 0 0) in 50 mM $H_2SO_4$ solution at −1400 mV. The orientation of Pb(1 0 0) substrate is indicated by arrows.

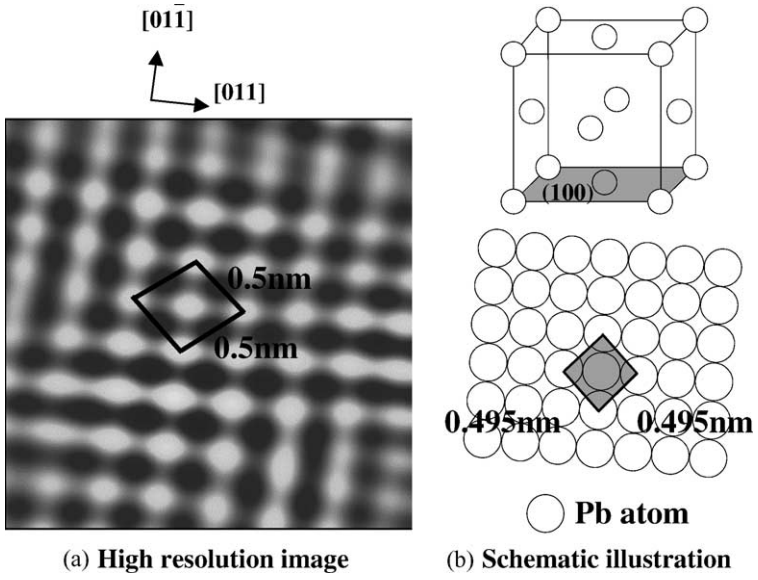


Fig. 4. (a) EC-AFM high resolution image (3 nm × 3 nm) on Pb(1 0 0) in 50 mM $H_2SO_4$ solution at −1400 mV. The orientation of Pb(1 0 0) substrate is indicated by arrows. (b) Schematic illustration of image (a).

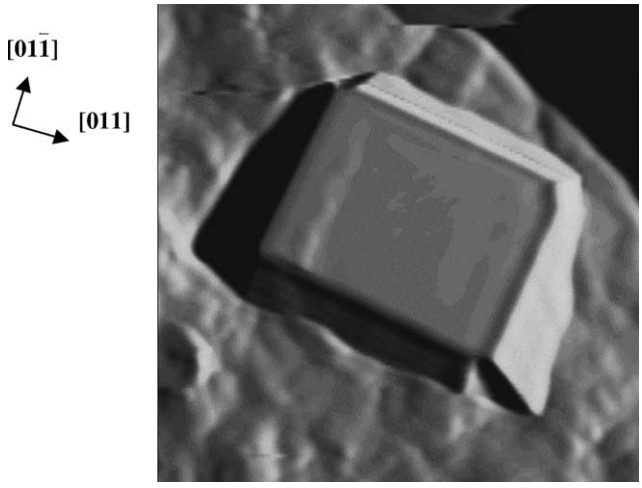


Fig. 5. EC-AFM morphological image (2.5 μm × 2.5 μm) on Pb(1 0 0) in 50 mM $H_2SO_4$ solution at 0 mV. The orientation of Pb(1 0 0) substrate is indicated by arrows.

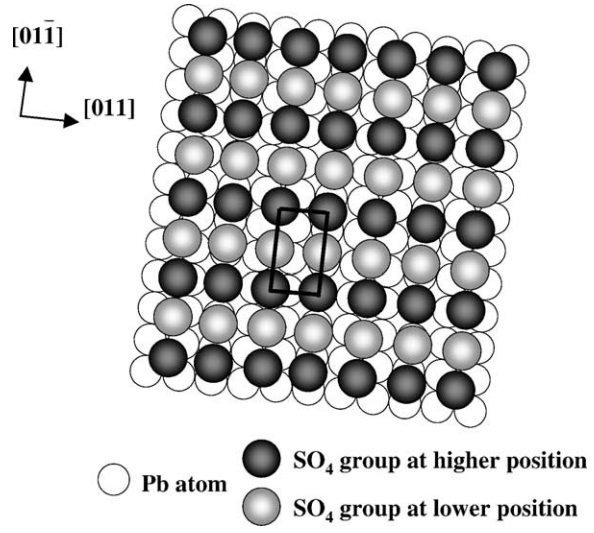


Fig. 7. Schematic illustration of orientation relationship between Pb atoms in Fig. 4 and $SO_4$ groups in Fig. 6. The orientation of Pb(1 0 0) substrate is indicated by arrows.

Superior) and Milli-Q water. All of the experiments are performed at room temperature.

## 3. Results and discussion

### 3.1. Cyclic voltammogram

Fig. 2 shows cyclic voltammograms (CVs) for Pb(1 0 0) and Pb(1 1 1) in 50 mM $H_2SO_4$ solution with sweep rate of 1 mV $s^{-1}$. In the positive scan, there are oxidation peaks at −850 mV, which correspond to the reaction of $Pb + SO_4^{2-} \rightarrow PbSO_4 + 2e^-$. Reversing the potential toward negative at −650 mV, there are cathodic peaks at −1000 mV, which correspond to the reaction of $PbSO_4 + 2e^- \rightarrow Pb + SO_4^{2-}$. These CVs agree well with the one for the lead sheet samples [2].

### 3.2. EC-AFM observation on Pb(1 0 0)

Fig. 3 shows an EC-AFM morphological image (5 μm × 5 μm) on Pb(1 0 0) in 50 mM $H_2SO_4$ solution at −1400 mV. On the terrace in Fig. 3, a filtered high resolution EC-AFM image (3 nm × 3 nm) is obtained as shown in Fig. 4a. We can recognize the spots having four-fold symmetry with interatomic distance of 0.35 nm. It corresponds well to a bare and unreconstructed Pb(1 0 0) (1 × 1) structure as

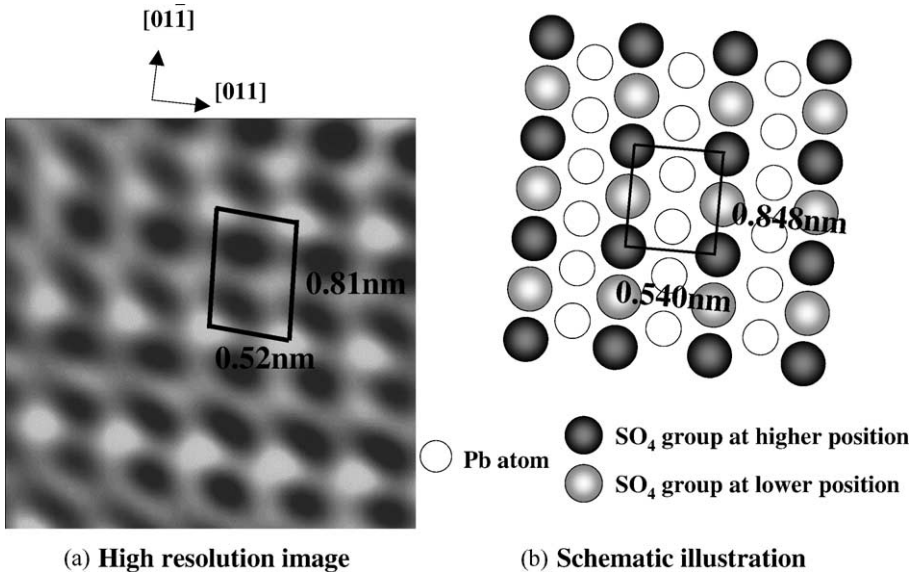


Fig. 6. (a) EC-AFM high resolution image (3 nm × 3 nm) on Pb(1 0 0) in 50 mM $H_2SO_4$ solution at 0 mV. The orientation of Pb(1 0 0) substrate is indicated by arrows. (b) Schematic illustration of image (a).

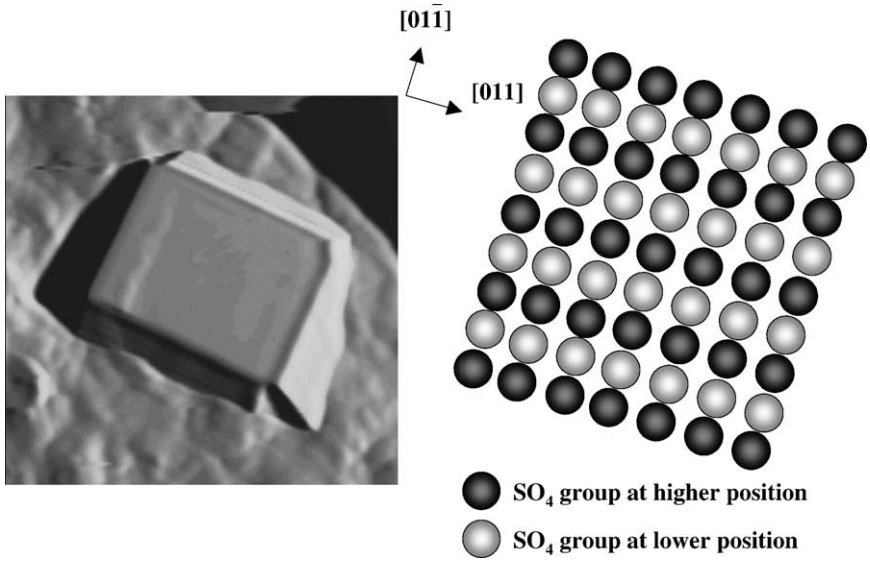


Fig. 8. Orientation relationship between Fig. 5 and $SO_4$ groups in Fig. 6. The orientation of Pb(1 0 0) substrate is indicated by arrows.

shown schematically in Fig. 4b. We have also succeeded in the observation of the growth of a $PbSO_4$ crystal on the Pb(1 0 0) electrode when the potential is stepped from −1400 to 0 mV, as shown in Fig. 5 (2.5 μm × 2.5 μm). On the top plane of the $PbSO_4$ crystal in Fig. 5, a filtered high resolution EC-AFM image (3 nm × 3 nm) is obtained as shown in Fig. 6a. We can recognize the spots, which have two-fold symmetry with interatomic distances of 0.41 and 0.52 nm. This superlattice corresponds to the protuberances by $SO_4$ groups of the unreconstructed $PbSO_4$(0 0 1) (1 × 1) structure (Fig. 6b). Fig. 7 shows a schematic illustration of orientation relationship between Pb atoms in Fig. 4 and $SO_4$ groups in Fig. 6. We found that the atomic rows along the [1 0 0] and [0 1 0] direction of $PbSO_4$(0 0 1) surface were parallel with those along the [0 1 1] and [0 1$\bar{1}$] direction of Pb(1 0 0) substrate, respectively. Fig. 8 shows an orientation relationship between Fig. 5 and $SO_4$ groups in Fig. 6. We also found that the top plane of $PbSO_4$ crystal in Fig. 5 is surrounded by [0 1 1] and [0 1$\bar{1}$] steps.

### 3.3. EC-AFM observation on Pb(1 1 1)

Fig. 9a shows a filtered high resolution EC-AFM image (2.5 nm × 2.5 nm). We can recognize the spots having three-fold symmetry with interatomic distance of 0.36 nm. It corresponds well to a bare and unreconstructed Pb(1 1 1)

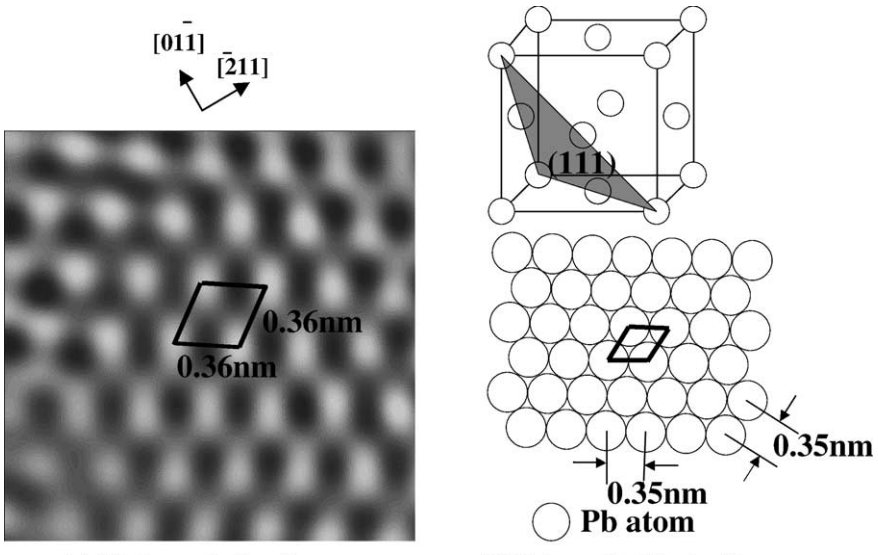


Fig. 9. (a) EC-AFM high resolution image (2.5 nm × 2.5 nm) on Pb(1 1 1) in 50 mM $H_2SO_4$ solution at −1400 mV. The orientation of Pb(1 1 1) substrate is indicated by arrows. (b) Schematic illustration of image (a).

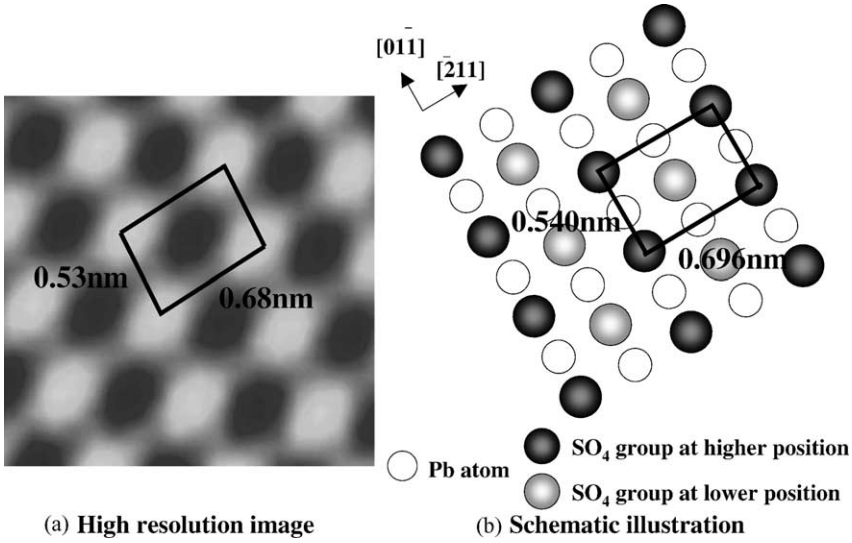


Fig. 10. (a) EC-AFM high resolution image (2.1 nm × 2.1 nm) on Pb(1 1 1) in 50 mM $H_2SO_4$ solution at 0 mV. The orientation of Pb(1 1 1) substrate is indicated by arrows. (b) Schematic illustration of image (a).

(1 × 1) structure as shown schematically in Fig. 9b. We have also succeeded in the observation of the growth of a $PbSO_4$ crystal on the Pb(1 1 1) electrode when the potential is stepped from −1400 to 0 mV, as shown in Fig. 12 (2.5 μm × 2.5 μm). On the top plane of the $PbSO_4$ crystal in Fig. 12, a filtered high resolution EC-AFM image (2.1 nm × 2.1 nm) is obtained as shown in Fig. 10a. We can recognize the spots, which have two-fold symmetry with interatomic distances of 0.53 and 0.68 nm. This superlattice corresponds to the protuberances by $SO_4$ groups (only at higher position) of the unreconstructed $PbSO_4$(1 0 0) (1 × 1) structure (Fig. 10b). Fig. 11 shows a schematic illustration of the orientation relationship between Pb atoms in Fig. 9 and $SO_4$ groups (only at higher position) in Fig. 10. We found that the atomic rows along the [0 1 0] and [0 0 1] direction of $PbSO_4$ (1 0 0) surface were parallel with those along the [0 1 $\bar{1}$] and [$\bar{2}$1 1] direction of Pb(1 1 1) substrate, respectively. Fig. 12 shows an orientation relationship between the

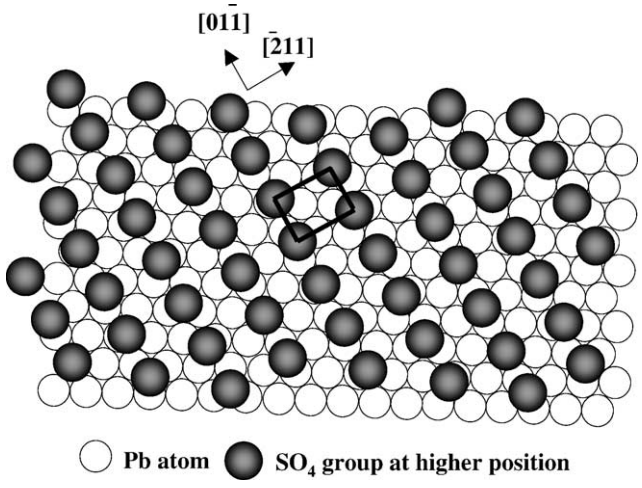


Fig. 11. Schematic illustration of orientation relationship between Pb atoms in Fig. 9 and $SO_4$ groups at higher position in Fig. 10. The orientation of Pb(1 1 1) substrate is indicated by arrows.

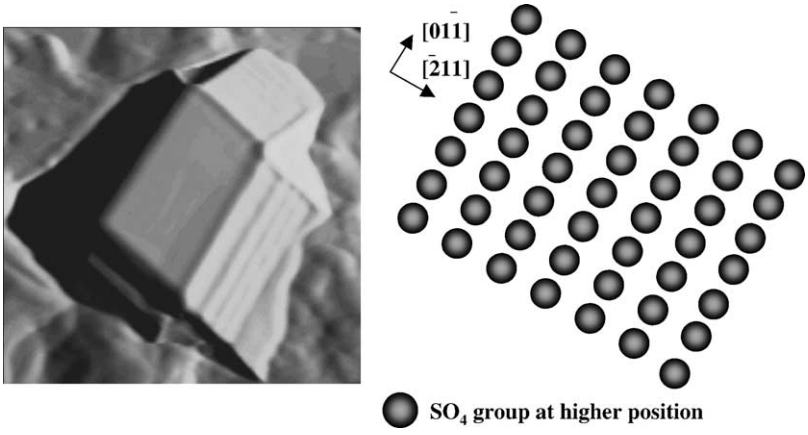


Fig. 12. EC-AFM morphological image (2.5 μm × 2.5 μm) on Pb(1 1 1) in 50 mM $H_2SO_4$ solution at 0 mV and orientation relationship between this image and $SO_4$ groups at higher position Fig. 10. The orientation of Pb(1 1 1) substrate is indicated by arrows.

EC-AFM morphological image of a $PbSO_4$ crystal on the Pb(1 1 1) electrode and $SO_4$ groups (only at higher position) in Fig. 10. We also found that the top plane of the $PbSO_4$ crystal in Fig. 12 is surrounded by [0 1$\bar{1}$] and [$\bar{2}$1 1] steps.

## 4. Conclusion

Pb(1 0 0) and Pb(1 1 1) single crystals in 50 mM $H_2SO_4$ aqueous solution have been investigated by in situ EC-AFM under potential control. We have succeeded in observation on high resolution images of Pb(1 0 0) and Pb(1 1 1) single crystals, as well as high resolution and morphological images of $PbSO_4$ crystals formed on the Pb single crystals. The following conclusions were derived from Section 3.

1. We found that the top face of $PbSO_4$ crystals formed on Pb(1 0 0) is $PbSO_4$(0 0 1), while that on Pb(1 1 1) is $PbSO_4$(1 0 0).
2. We also found that the atomic rows along the [1 0 0] and [0 1 0] direction of $PbSO_4$ (0 0 1) surface were parallel with those along the [0 1 1] and [0 1$\bar{1}$] direction of Pb(1 0 0) substrate, while those along the [0 1 0] and [0 0 1] direction of $PbSO_4$ (1 0 0) surface were parallel with those along the [0 1$\bar{1}$] and [$\bar{2}$1 1] direction of Pb(1 1 1) substrate.

## Acknowledgements

This study was partly supported by Industrial Technology Research Grant Program (ID number: 01B60015C) in 2001 from New Energy and Industrial Technology Development Organization (NEDO) of Japan.

## References

[1] Y. Yamaguchi, M. Shiota, Y. Nakayama, N. Hirai, S. Hara, J. Power Sources 85 (2000) 22.
[2] Y. Yamaguchi, M. Shiota, Y. Nakayama, N. Hirai, S. Hara, J. Power Sources 93 (2001) 104.
[3] M. Shiota, Y. Yamaguchi, Y. Nakayama, K. Adachi, S. Taniguchi, N. Hirai, S. Hara, J. Power Sources 95 (2001) 203.
[4] Y. Yamaguchi, M. Shiota, Y. Nakayama, N. Hirai, S. Hara, J. Power Sources 102 (2001) 156.
[5] I. Ban, Y. Yamaguchi, Y. Nakayama, N. Hirai, S. Hara, J. Power Sources 107 (2002) 167–172.
[6] A.A. Gewirth, B.K. Niece, Chem. Rev. 97 (1997) 1129–1162.
[7] K. Itaya, Prog. Surf. Sci. 58 (1998) 121–248.
[8] S.L. Yau, F.R.F. Fan, T.P. Moffat, A.J. Bard, J. Phys. Chem. 98 (1994) 5493.
[9] T. Suzuki, T. Yamada, K. Itaya, J. Phys. Chem. 100 (1996) 8954.
[10] S. Ando, T. Suzuki, K. Itaya, J. Electroanal. Chem. 431 (1997) 277.
[11] N. Hirai, H. Okada, S. Hara, ISIJ Int. 40 (2000) 702.
[12] K. Uosaki, K. Konishi, M. Koinuma, Langmuir 13 (1997) 3557.